

# HQET chromomagnetic interaction at two loops

A. Czarnecki

Institut für Theoretische Teilchenphysik, Universität Karlsruhe,  
D-76128 Karlsruhe, Germany

A. G. Grozin

Budker Institute of Nuclear Physics, Novosibirsk 630090, Russia

## Abstract

We present the coefficient of the chromomagnetic interaction operator, the only unknown coefficient in the Heavy Quark Effective Theory (HQET) lagrangian up to the  $1/m$  level, with the two-loop accuracy by matching scattering amplitudes of an on-shell heavy quark in an external field in full QCD and HQET, and obtain the two-loop anomalous dimension of this operator in HQET.

## 1 Introduction

The leading order HQET lagrangian [1]

$$L_0 = \bar{Q}_v i v D Q_v \quad (1)$$

has a unit coefficient by construction (here  $Q_v = \not{v} Q$  is a static quark field with velocity  $v$ ). At the  $1/m$  level two new terms appear [2, 3]

$$L = L_0 + \frac{C_k(\mu)}{2m} \bar{Q}_v ((vD)^2 - D^2) Q_v + \frac{C_m(\mu)}{4m} \bar{Q}_v G_{\mu\nu} \sigma^{\mu\nu} Q_v \quad (2)$$

(where the composite operators are normalized at the scale  $\mu$ ). For the coefficient of the kinetic-energy operator

$$C_k(\mu) = 1 \quad (3)$$

holds in all orders of perturbation theory, due to reparametrization invariance of HQET [4, 5, 6]. Only the coefficient  $C_m(\mu)$  of the chromomagnetic interaction operator is not known exactly. It can be found by matching scattering amplitudes of an on-shell heavy quark in an external chromomagnetic field in QCD and HQET up to  $1/m$  terms. This was done in [2] at the one-loop level; the one-loop anomalous dimension of the chromomagnetic interaction operator is

therefore known [2, 3]. It is natural to perform matching at  $\mu \approx m$ , where  $C_m(\mu)$  contains no large logarithm. Renormalization group can be used to obtain  $C_m$  at  $\mu \ll m$ :

$$C_m(\mu) = C_m(m) \exp \left( - \int_{\alpha_s(m)}^{\alpha_s(\mu)} \frac{\gamma_m(\alpha)}{2\beta(\alpha)} \frac{d\alpha}{\alpha} \right). \quad (4)$$

Two-loop anomalous dimension  $\gamma_m = \frac{d \log Z_m}{d \log \mu} = \gamma_1 \frac{\alpha_s}{4\pi} + \gamma_2 \left( \frac{\alpha_s}{4\pi} \right)^2 + \dots$  and  $\beta$ -function  $\beta = -\frac{1}{2} \frac{d \log \alpha_s}{d \log \mu} = \beta_1 \frac{\alpha_s}{4\pi} + \beta_2 \left( \frac{\alpha_s}{4\pi} \right)^2 + \dots$  should be used together with one-loop terms in  $C_m(m) = 1 + C_1 \frac{\alpha_s(m)}{4\pi} + \dots$  [2]. Chromomagnetic interaction is the only term violating the heavy-quark spin symmetry [7] at the  $1/m$  level. Numerous applications of the lagrangian (1–2) are reviewed in [8].

In this paper, we obtain  $C_m(\mu)$  at two loops from QCD/HQET matching. We consider scattering amplitude of an on-shell heavy quark with the initial momentum  $p_1 = mv$  and a final momentum  $p_2$  in a weak external field  $A_\mu^a$  to the linear order in  $q = p_2 - p_1$ . Similarly to [2], we use dimensional regularization (in  $d = 4 - 2\varepsilon$  dimensions) and the background field formalism [10] in which the combination  $gA_\mu^a$  is not renormalized. We consider QCD with  $n_l$  massless flavours and a single heavy flavour  $Q$ ; the effect of a massive flavour with a different mass will be considered elsewhere. There are two possible effective theories: with loops of the heavy flavour  $Q$  and without such loops. Matching on-shell matrix elements produces finite results in both theories, in contrast to the case of a heavy-light current [9]. The HQET diagrams contain no scale and hence vanish in dimensional regularization, except for those with a massive quark loop (Section 2). QCD on-shell diagrams were independently calculated with the REDUCE [11, 12] package RECURSOR [13] and a FORM [14] package [15] (Section 3). Comparing the HQET and QCD matrix elements, we obtain the matching coefficient  $C_m(m)$  and its anomalous dimension  $\gamma$  (Section 4).

## 2 HQET calculation

The scattering matrix element of an on-shell quark in HQET up to  $1/m$  level has the structure

$$M = \bar{u}_v(q) g A_\mu^a t^a \left( v^\mu + C_k Z_k^{-1} \tilde{\varepsilon} \frac{q^\mu}{2m} + C_m Z_m^{-1} \tilde{\mu} \frac{[\gamma^\mu, \not{q}]}{4m} \right) u_v(0), \quad (5)$$

where  $qv = 0$ ;  $\tilde{\varepsilon} = \tilde{Z}_Q \tilde{\varepsilon}_0$ ,  $\tilde{\mu} = \tilde{Z}_Q \tilde{\mu}_0$ ;  $\tilde{\varepsilon}_0$  and  $\tilde{\mu}_0$  are the bare proper vertex functions of the unrenormalized operators  $\bar{Q}_v ((vD)^2 - D^2) Q_v$  and  $\bar{Q}_v G_{\mu\nu} \sigma^{\mu\nu} Q_v$ . In HQET with  $n_l$  massless flavours in loops, all loop corrections vanish because they contain no scale:  $\tilde{Z}_Q = 1$ ,  $\tilde{\varepsilon}_0 = 1$ ,  $\tilde{\mu}_0 = 1$ .

In HQET with the heavy flavour  $Q$  in loops, the on-shell wave-function renormalization constant was found in [9]:

$$\tilde{Z}_Q = 1 - C_F T_F \frac{g_0^4 m^{-4\varepsilon}}{(4\pi)^d} I_0^2 \frac{(d-1)(d-2)(d-6)}{2(d-5)(d-7)}, \quad (6)$$

$$I_0 = \frac{1}{\pi^{d/2}} \int \frac{d^d k}{1 - (v+k)^2} = \frac{2}{d-2} \Gamma(\varepsilon); \quad (7)$$

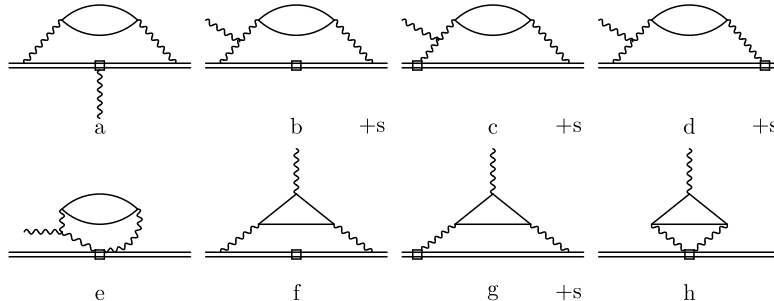


Figure 1: Diagrams for  $\tilde{\varepsilon}_0$ ; +s means adding the mirror-symmetric diagram.

Diagrams for  $\tilde{\varepsilon}_0$  are shown in Fig. 1. We consider  $A_\mu^a v^\mu = 0$ , and therefore diagrams in which the background field is attached to the leading-order HQET vertex  $igt^a v^\mu$  do not contribute. Diagrams in which the background field is attached to a four-leg  $1/m$  vertex do not depend on  $q$  and do not contribute to the structure linear in  $q$ . The diagrams Fig. 1e, h have zero colour factor. A method of calculation of scalar integrals in such diagrams was proposed in [9]: we average over directions of  $v$  in scalar integrals and obtain

$$\overline{(vk)^n} = \frac{\Gamma(\frac{n+1}{2})}{\Gamma(\frac{1}{2})} \frac{\Gamma(\frac{d}{2})}{\Gamma(\frac{d+n}{2})} (k^2)^{n/2} \quad (8)$$

for even  $n$  (positive or negative) and 0 for odd  $n$ . After that, two-loop massive bubble integrals remain. An explicit formula for them can be found in [16]. We perform calculations in an arbitrary covariant gauge, and check that the sum of diagrams is gauge-invariant. Only the diagram Fig. 1a contains the colour structure  $C_F T_F$ ; it is easy to see that this contribution is exactly compensated by  $\tilde{Z}_Q$  (6). In order to calculate  $\tilde{\varepsilon}_0$ , we can contract the diagrams with  $q$  in the polarization index of the external gluon, and extract the  $q^2$  part. In the background field formalism, such external-gluon insertions produce the difference of the propagators with the original momentum and the momentum shifted by  $q$  (after separating colour factors). Let's consider the diagrams Fig. 1c, d, g first. Most of the terms in the sum cancel each other, leaving the difference of two terms: the diagram without the external gluon, and the same diagram with the heavy-quark momentum shifted by  $q$ . This shift does not influence the propagator; the kinetic energy vertex contains a term linear in  $q$ , which vanishes after the loop integrations. The sum of the diagrams Fig. 1b, f gives a similar difference of two diagrams without the external gluon. The difference of the two-leg kinetic energy vertices now contains a  $q^2$  term, which is multiplied by

the same integral as in (6). Finally, we obtain

$$\tilde{\varepsilon} = 1. \quad (9)$$

This fact is crucial for the proof of (3). Note that the ‘‘all-order’’ proof of the reparametrization invariance [6] ignores all massive loops in HQET (of the external heavy flavour or any other massive quark) and therefore is valid up to the one-loop level only.

In the case of  $\tilde{\mu}_0$ , the diagrams Fig. 1b, f do not exist. The colour factors of Fig. 1e, h no longer vanish. Again, the only  $C_F T_F$  contribution of Fig. 1a is compensated by  $\tilde{Z}_Q$  and we obtain

$$\tilde{\mu} = 1 + C_A T_F \frac{g_0^4 m^{-4\varepsilon}}{(4\pi)^d} I_0^2 \frac{(d-2)(d^2-9d+16)}{4(d-5)(d-7)}. \quad (10)$$

### 3 QCD calculation

The scattering matrix element of an on-shell quark in a weak external field has the structure

$$M = \bar{u}(p_2) g A_\mu^{a t^\alpha} \left( \varepsilon(q^2) \frac{(p_1 + p_2)^\mu}{2m} + \mu(q^2) \frac{[\gamma^\mu, \not{q}]}{4m} \right) u(p_1). \quad (11)$$

Up to the linear terms in  $q$  it is determined by the total quark colour charge  $\varepsilon = Z_Q \varepsilon_0(0) = 1$  and chromomagnetic moment  $\mu = Z_Q \mu_0(0)$ . The on-shell wave-function renormalization  $Z_Q$  was obtained in [17]. Let us see why  $\varepsilon = 1$ . Diagrams for the bare proper vertex  $\Lambda_0^\mu$  in the constant background field  $A_\mu$  can be obtained from the diagrams for the bare mass operator  $\Sigma_0(p)$  by shifting  $p$ :  $\Sigma_0(p+A) = \Sigma_0(p) - \Lambda_0^\mu A_\mu$ . The term  $\varepsilon_0$  is separated by the  $\gamma$ -matrix projector  $\varepsilon_0 = 1 + \frac{1}{4} \text{Tr} \Lambda_0^\mu v_\mu (\not{v} + 1)$ . On the mass shell,  $\frac{1}{4} \text{Tr} (\Sigma_0(mv+A) - \Sigma_0(mv)) (\not{v} + 1) = (1 - Z_Q^{-1}) v A$ . This gives  $\varepsilon_0 = Z_Q^{-1}$ . This argument is valid for both an abelian and a nonabelian background field  $A$ .

We calculate bare proper vertices  $\varepsilon_0$ ,  $\mu_0$  on the renormalized mass shell. Therefore, it is convenient to use the pole mass  $m$  in the lagrangian, and to incorporate the vertex produced by the mass counterterm  $\Delta m$  [16]. Diagrams for the proper vertex can be obtained from those for the mass operator by inserting the background field vertex in all possible ways (Fig. 2). Using integration by parts recurrence relations [16, 17], all two-loop on-shell integrals can be reduced to  $I_0^2$  and

$$\begin{aligned} I_1 &= \frac{1}{\pi^d} \int \frac{d^d k d^d l}{(-k^2)(-l-k)^2(1-(v+l)^2)} \\ &= \frac{4(2d-7)}{(d-3)(3d-8)(3d-10)} \frac{\Gamma^2(1-\varepsilon)\Gamma(1+2\varepsilon)\Gamma(1-4\varepsilon)}{\Gamma(1+\varepsilon)\Gamma(1-2\varepsilon)\Gamma(1-3\varepsilon)} \Gamma^2(\varepsilon), \\ I_2 &= \frac{1}{\pi^d} \int \frac{d^d k d^d l}{(1-(v+k)^2)(1-(v+l)^2)(1-(v+k+l)^2)} \\ &= \frac{3(d-2)^2(5d-18)}{2(d-3)(3d-8)(3d-10)} I_0^2 - 2 \frac{d-4}{2d-7} I_1 - \frac{16(d-4)^2}{(3d-8)(3d-10)} I(\varepsilon), \end{aligned} \quad (12)$$

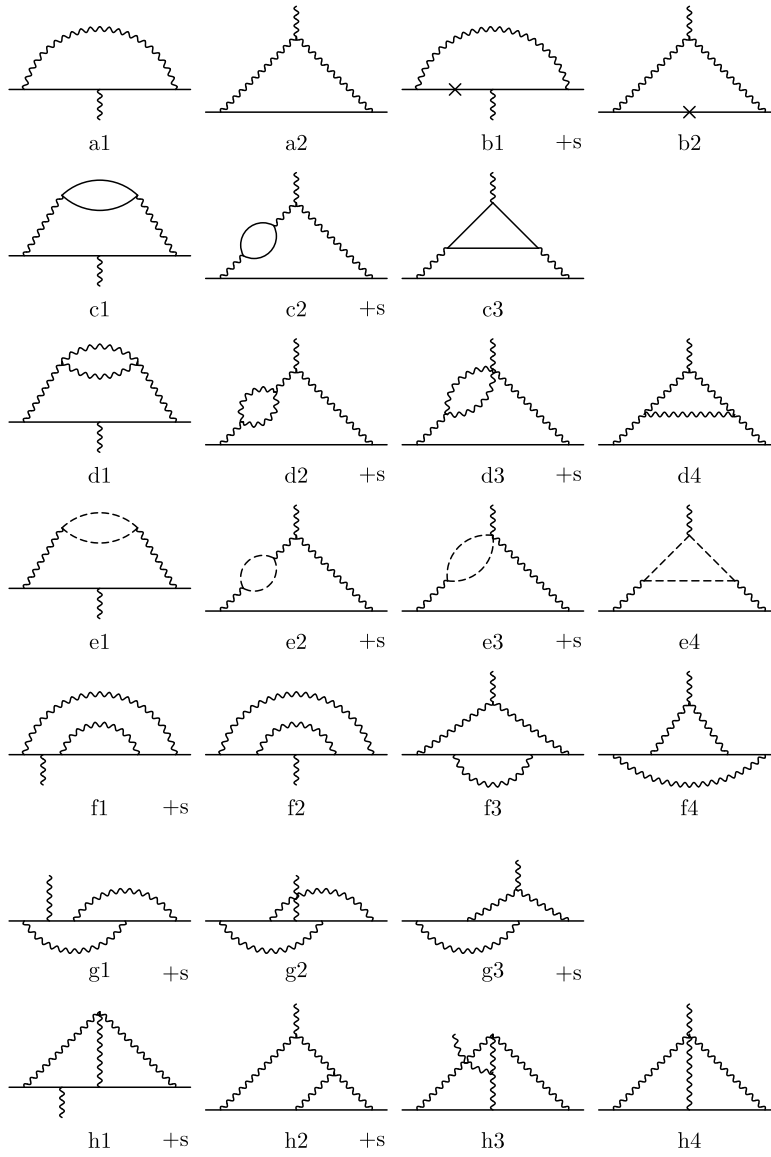


Figure 2: Diagrams for the QCD proper vertex.

where [18, 13]

$$I(\varepsilon) = I + O(\varepsilon), \quad I = \pi^2 \log 2 - \frac{3}{2}\zeta(3). \quad (13)$$

The diagrams Fig. 2c with massless quarks (colour structures  $C_F T_F n_l$  and  $C_A T_F n_l$ ) and Fig. 2d, e contain only  $I_1$ . The integral  $I_2$  is contained only in Fig. 2c with the heavy quark (colour structures  $C_F T_F$  and  $C_A T_F$ ) and Fig. 2g. The diagram Fig. 2h3 has zero colour factor.

We perform all calculations in an arbitrary covariant gauge, and check that the  $d$ -dimensional results for  $\varepsilon_0$  and  $\mu_0$  are gauge-invariant. We check that  $\varepsilon_0 = Z_Q^{-1}$ ; the same equality holds if we use colour factors for an abelian background fields in  $\varepsilon_0$ . Moreover, this is true for each group of diagrams obtained from a single diagram for the mass operator: the sum of these diagrams, with each set of colour factors, gives the contribution of the original diagram to  $Z_Q^{-1}$ . This provides a strong check of our procedures. The programs for calculating  $\mu_0$  are obtained by replacing only the  $\gamma$ -matrix projector and hence are reliable. If we use colour factors for an abelian background field, we reproduce the heavy-quark magnetic moment [19]; if the dynamical gauge field is also abelian, the classic result for the QED electron magnetic moment [20] is reproduced (in dimensional regularization, it was discussed in [21]). In view of all these checks, we are confident in our final result for the heavy-quark chromomagnetic moment.

The full  $d$ -dimensional result is presented in the Appendix. Expanding it in  $\varepsilon$  and re-expressing it via  $\alpha_s(\mu)$ , we obtain

$$\begin{aligned} \mu = 1 + \frac{\alpha_s(\mu)}{4\pi} e^{-2L\varepsilon} \left( 1 - \frac{\alpha_s}{4\pi\varepsilon} \beta_1 \right) & \left[ 2C_F(1 + 4\varepsilon) + C_A \left( \frac{1}{\varepsilon} + 2 + \frac{\pi^2}{12}\varepsilon + 2\varepsilon \right) \right] \\ + \left( \frac{\alpha_s}{4\pi} \right)^2 e^{-4L\varepsilon} & \left[ C_F^2 \left( -8I + \frac{20}{3}\pi^2 - 31 \right) + C_F C_A \left( \frac{28}{3} \frac{1}{\varepsilon} + \frac{4}{3} I + \frac{4}{3}\pi^2 + \frac{605}{9} \right) \right. \\ + C_A^2 & \left( \frac{7}{3} \frac{1}{\varepsilon^2} + \frac{101}{9} \frac{1}{\varepsilon} + \frac{4}{3} I - \frac{3}{2}\pi^2 + \frac{1057}{27} \right) \\ + C_F T_F n_l & \left( -\frac{8}{3} \frac{1}{\varepsilon} - \frac{196}{9} \right) + C_A T_F n_l \left( -\frac{2}{3} \frac{1}{\varepsilon^2} - \frac{37}{9} \frac{1}{\varepsilon} - \frac{5}{9}\pi^2 - \frac{371}{27} \right) \\ + C_F T_F & \left( -\frac{8}{3} \frac{1}{\varepsilon} - \frac{16}{3}\pi^2 + \frac{380}{9} \right) + C_A T_F \left( -\frac{4}{3} \frac{1}{\varepsilon^2} - \frac{8}{3} \frac{1}{\varepsilon} + \frac{8}{9}\pi^2 - \frac{370}{27} \right) \left. \right], \quad (14) \end{aligned}$$

where  $L = \log m/\mu$ ,  $\beta_1 = \frac{11}{3}C_A - \frac{4}{3}T_F n_f$ ,  $n_f = n_l + 1$ .

## 4 Results

The coefficients  $C_k$ ,  $C_m$  in the HQET lagrangian (2) are tuned in such a way that the full QCD matrix element (11), expanded to linear terms in  $q$ , is equal to the HQET matrix element (5). Infrared (or on-shell) singularities are the same in both theories. QCD and HQET spinors are related by [8]  $u(p_1) = u_v(0)$ ,

$u(p_2) = \left(1 + \frac{\not{h}}{2m}\right) u_v(q)$ ; the extra term with  $\not{h}$  should only be taken into account in zeroth order terms, but then it vanishes.

We consider HQET with  $n_l$  light flavours in loops first. Comparing the structure  $q^\mu$ , we obtain  $Z_k^{-1}C_k = 1$ , and hence  $C_k(\mu) = 1$  (3). Comparing the structure  $[\gamma^\mu, \not{q}]$ , we obtain  $Z_m^{-1}C_m = \mu/\bar{\mu}$ . We find  $Z_m$  from the requirement that  $C_m$  is finite. Terms  $1/\varepsilon^2$  in it satisfy the consistency condition which is necessary for the anomalous dimension to be finite at  $\varepsilon \rightarrow 0$ . Terms  $1/\varepsilon$  give the anomalous dimension

$$\gamma_m = 2C_A \frac{\alpha_s}{4\pi} + \frac{4}{9}C_A(17C_A - 13T_F n_l) \left(\frac{\alpha_s}{4\pi}\right)^2. \quad (15)$$

The chromomagnetic interaction coefficient at  $\mu = m$  is

$$\begin{aligned} C_m(m) = & 1 + 2(C_F + C_A) \frac{\alpha_s(m)}{4\pi} + \left[ C_F^2 \left( -8I + \frac{20}{3}\pi^2 - 31 \right) \right. \\ & + C_F C_A \left( \frac{4}{3}I + \frac{4}{3}\pi^2 + \frac{269}{9} \right) + C_A^2 \left( \frac{4}{3}I - \frac{17}{9}\pi^2 + \frac{805}{27} \right) \\ & + C_F T_F n_l \left( -\frac{100}{9} \right) + C_A T_F n_l \left( -\frac{4}{9}\pi^2 - \frac{299}{27} \right) \\ & \left. + C_F T_F \left( -\frac{16}{3}\pi^2 + \frac{476}{9} \right) + C_A T_F \left( \pi^2 - \frac{298}{27} \right) \right] \left( \frac{\alpha_s}{4\pi} \right)^2. \end{aligned} \quad (16)$$

With  $N_c = 3$  colours, its numerical value is

$$C_m(m) = 1 + \frac{16}{3} \frac{\alpha_s(m)}{\pi} + (21.79 - 1.91n_l) \left( \frac{\alpha_s}{\pi} \right)^2. \quad (17)$$

The two-loop correction is large. The exact two-loop coefficient at  $n_l = 4$  is 40% less than the expectation based on the naive nonabelianization [9], i. e. it is not particularly accurate, but predicts the correct sign and order of magnitude. The heavy-quark loop contributes merely  $-0.10$  to the bracket in (17).

If we now include  $Q$ -loops in HQET, we still have  $C_k(\mu) = 1$  (3). The anomalous dimension (15) now contains  $n_f = n_l + 1$  instead of  $n_l$ . The chromomagnetic interaction coefficient (16) has the coefficient of  $C_A T_F$  equal to  $\frac{10}{9}\pi^2 - \frac{227}{27}$ , leading to 22.14 in the bracket in (17).

Our main results are the anomalous dimension (15) and the chromomagnetic interaction coefficient at  $\mu = m$  (16). If  $L = \log m/\mu$  is not very large, the best approximation to  $C_m(\mu)$  is the exact two-loop matching formula

$$C_m(\mu) = 1 + (C_1 - \gamma_1 L) \frac{\alpha_s(m)}{4\pi} + [C_2 - (C_1 \gamma_1 + \gamma_2) L + \gamma_1 (\gamma_1 - \beta_1) L^2] \left( \frac{\alpha_s}{4\pi} \right)^2, \quad (18)$$

in which all terms  $(\alpha_s/\pi)^2 L^{2,1,0}$  are taken into account, but  $(\alpha_s/\pi)^3 L^3$  and other higher order terms are dropped. Otherwise, it is better to sum leading

and subleading logarithms using (4):

$$C_m(\mu) = \left( \frac{\alpha_s(\mu)}{\alpha_s(m)} \right)^{-\gamma_1/(2\beta_1)} \left[ 1 + C_1 \frac{\alpha_s(m)}{4\pi} - \frac{\beta_1\gamma_2 - \beta_2\gamma_1}{2\beta_1^2} \frac{\alpha_s(\mu) - \alpha_s(m)}{4\pi} \right]. \quad (19)$$

These results can be applied to all cases of the spin symmetry violation, such as  $D-D^*$  and  $B-B^*$  splittings,  $1/m$  corrections in  $B \rightarrow D$  and  $B \rightarrow D^*$  semileptonic decays, etc. [8].

In the course of this work, we were informed by M. Neubert about the ongoing calculation of the two-loop anomalous dimension of the chromomagnetic interaction operator by a completely different method [22]. Our result (15) agrees with [22].

**Acknowledgements.** We are grateful to M. Neubert for communicating the result of [22] before publication, and to D. J. Broadhurst for numerous fruitful discussions of HQET and methods of multiloop calculations. A. C.'s research was supported by the grant BMBF 057KA92P.



## A Heavy-quark chromomagnetic moment

The  $d$ -dimensional chromomagnetic moment has the form

$$\begin{aligned} \mu = 1 + \frac{g_0^2 m^{-2\epsilon}}{(4\pi)^{d/2}} \frac{1}{4} \frac{d-2}{d-3} [2(d-4)(d-5)C_F - (d^2 - 8d + 14)C_A] I_0 \\ + \frac{g_0^4 m^{-4\epsilon}}{(4\pi)^d} \sum_{i,j} a_{ij} C_i J_j, \end{aligned}$$

where the colour structures are  $C_1 = C_F^2$ ,  $C_2 = C_F C_A$ ,  $C_3 = C_A^2$ ,  $C_4 = C_F T_F n_l$ ,  $C_5 = C_A T_F n_l$ ,  $C_6 = C_F T_F$ ,  $C_7 = C_A T_F$  and

$$\begin{aligned} J_0 = \frac{(d-2)I_0^2}{16(d-1)(d-3)^2(d-4)^2(d-5)(d-6)(d-7)}, \\ J_1 = \frac{I_1}{16(d-1)(d-3)(d-4)(2d-7)}, \quad J_2 = \frac{I_2}{16(d-1)(d-4)^2(d-6)} \end{aligned}$$

are chosen in such a way that the coefficients  $a_{ij}$  are polynomial in  $d$ . L<sup>A</sup>T<sub>E</sub>X source of the following equation, presenting all nonvanishing coefficients  $a_{ij}$ , was generated by a REDUCE program using the package RLFI by R. Liska (see [11, 12]):

$$\begin{aligned} a_{11} &= 4(d-5)(d-6)(d-7)(d^8 - 32d^7 + 460d^6 - 3828d^5 + 19940d^4 - 66032d^3 \\ &\quad + 135065d^2 - 155640d + 77356) \\ a_{12} &= -16(2d-7)(2d^6 - 53d^5 + 557d^4 - 3005d^3 + 8828d^2 - 13450d + 8336) \\ a_{13} &= 8(d-6)(2d^6 - 60d^5 + 682d^4 - 3871d^3 + 11723d^2 - 18066d + 11120) \\ a_{21} &= -2(d-6)(d-7)(2d^9 - 72d^8 + 1175d^7 - 11329d^6 + 70628d^5 - 293546d^4 \\ &\quad + 809949d^3 - 1426799d^2 + 1454100d - 652948) \\ a_{22} &= 4(16d^7 - 474d^6 + 5777d^5 - 37896d^4 + 145361d^3 - 327378d^2 + 402044d \\ &\quad - 208160) \\ a_{23} &= -4(d-6)(5d^6 - 146d^5 + 1625d^4 - 9065d^3 + 27085d^2 - 41398d + 25424) \\ a_{31} &= (d-6)(d-7)(d^9 - 35d^8 + 557d^7 - 5259d^6 + 32250d^5 - 132396d^4 \\ &\quad + 362076d^3 - 633794d^2 + 642768d - 287288) \\ a_{32} &= -(3d-8)(6d^6 - 159d^5 + 1672d^4 - 9015d^3 + 26460d^2 - 40276d + 24928) \\ a_{33} &= 2(d-3)(d-6)(3d-8)(d^4 - 23d^3 + 176d^2 - 550d + 596) \\ a_{42} &= -64(d-2)(d-3)(d-4)^2(d^2 - 7d + 11) \\ a_{52} &= 4(d-3)(d-4)(3d-8)(2d^3 - 19d^2 + 57d - 56) \\ a_{61} &= 4(d-2)(d-3)(d-4)(d-7)(3d^5 - 85d^4 + 875d^3 - 4123d^2 + 8898d \\ &\quad - 7008) \\ a_{63} &= -8(d-4)(d^2 - 9d + 16)(d^3 - 13d^2 + 26d + 16) \\ a_{71} &= -(d-3)(d-4)(9d^7 - 290d^6 + 3822d^5 - 26680d^4 + 106477d^3 \\ &\quad - 242974d^2 + 294012d - 145896) \\ a_{73} &= 2(d-4)(3d-8)(d^4 - 16d^3 + 75d^2 - 96d - 28) \end{aligned}$$

## References

- [1] E. Eichten and B. Hill, Phys. Lett. **B234** (1990) 511.
- [2] E. Eichten and B. Hill, Phys. Lett. **B243** (1990) 427.
- [3] A. F. Falk, B. Grinstein, and M. E. Luke, Nucl. Phys. **B357** (1991) 185.
- [4] M. Luke and A. V. Manohar, Phys. Lett. **B286** (1992) 348.
- [5] Y.-Q. Chen, Phys. Lett. **B317** (1993) 421.
- [6] M. Finkemeier, H. Georgi, and M. McIrvin, Preprint HUTP-96/A053, hep-ph/9701243.
- [7] N. Isgur and M. B. Wise, Phys. Lett. **B232** (1989) 113; **B237** (1990) 527.
- [8] M. Neubert, Phys. Reports **245** (1994) 259.
- [9] D. J. Broadhurst and A. G. Grozin, Phys. Rev. **D52** (1995) 4082.
- [10] L. F. Abbot, Nucl. Phys. **B185** (1981) 189; Acta Phys. Pol. **B13** (1982) 33.
- [11] A. C. Hearn, REDUCE User's Manual, version 3.6, RAND Pub. CP78, Rev. 7/95 (1995).
- [12] A. G. Grozin, Using REDUCE in High Energy Physics, Cambridge University Press (1997).
- [13] D. J. Broadhurst, Zeit. Phys. **C54** (1992) 599.
- [14] J. A. M. Vermaseren, FORM User's Guide, Nikhef, Amsterdam (1990).
- [15] A. Czarnecki, Phys. Rev. Lett. **76** (1996) 4124.
- [16] N. Gray, D. J. Broadhurst, W. Grafe, and K. Schilcher, Zeit. Phys. **C48** (1990) 673.
- [17] D. J. Broadhurst, N. Gray, and K. Schilcher, Zeit. Phys. **C52** (1991) 111.
- [18] D. J. Broadhurst, Zeit. Phys. **C47** (1990) 115.
- [19] J. Fleischer and O. V. Tarasov, Phys. Lett. **B283** (1992) 129;  
D. J. Broadhurst and N. Gray, Preprint OUT-4102-36, The Open University (1992).
- [20] C. M. Sommerfield, Phys. Rev. **107** (1957) 328; Ann. Phys. **5** (1958) 26;  
A. Petermann, Helv. Phys. Acta **30** (1957) 407.
- [21] J. Fleischer and O. V. Tarasov, Comp. Phys. Comm. **71** (1992) 193;  
A. Czarnecki, Preprint AlbertaThy-18-92 (1992);  
A. Czarnecki and A. N. Kamal, Acta Phys. Pol. **B23** (1992) 1063.
- [22] G. Amorós, M. Beneke, and M. Neubert, Preprint CERN-TH/97-3, hep-ph/9701375.